

Received October 14, 2018, accepted November 6, 2018, date of publication January 1, 2019, date of current version January 29, 2019.

Digital Object Identifier 10.1109/ACCESS.2018.2888881

Collision-Free Fuzzy Formation Control of Swarm Robotic Cyber-Physical Systems Using a Robust Orthogonal Firefly Algorithm

SENDREN SHENG-DONG XU¹, (Senior Member, IEEE), HSU-CHIH HUANG²,
YU-CHIEH KUNG¹, AND SHAO-KANG LIN²

¹Graduate Institute of Automation and Control, National Taiwan University of Science and Technology, Taipei 10607, Taiwan

²Department of Electrical Engineering, National Ilan University, Yilan 26047, Taiwan

Corresponding author: Hsu-Chih Huang (hchuang@niu.edu.tw)

This work was supported by the Ministry of Science and Technology, Taiwan, under Grant MOST 107-2221-E-011-145, Grant MOST 106-2221-E-197-002, and Grant MOST 107-2221-E-197-028.

ABSTRACT This paper presents a collision-free fuzzy formation control strategy of swarm robotic cyber-physical systems (CPSs) using a robust orthogonal firefly algorithm (OFA). The classical FA is fused with the Taguchi method and the ranking mutation process to present a hybrid artificial intelligence. This computational intelligence is employed with the fuzzy theory to develop optimal cyber and cognition levels in swarm robotic CPS 5C architecture. With robotic sensors and actuators, the OFA-fuzzy-based cyber and cognition levels are incorporated with the smart connection, data-to-information conversion, and configuration levels to design a pragmatic swarm robotic CPS using system-on-a-programmable-chip technology. The broadcast distributed control strategy and potential field are employed to address the formation control problem of swarm robotic CPSs with obstacles. In the proposed swarm robotic CPS, the embedded central processing unit, operating system, networking intellectual property (IP), and robotic custom IPs are integrated into field-programmable gate array chips. The experimental results and comparisons with other methods show the merits of the proposed swarm robotic CPS in achieving collision-free distributed formation control.

INDEX TERMS CPS, collision-free, robust, firefly algorithm.

I. INTRODUCTION

To date, CPSs have been of interest in both academia and industry due to their potentially significant impact. A CPS is regarded as the next generation of engineering systems that integrates cyber computation, physical processes and networking via sensors and actuators in a feedback loop [1]–[3]. There are many software services, artificial intelligences and engineering methodologies involved in CPSs to achieve stability, reliability, performance and efficiency in application domains [4]. The overall design and deployment of a CPS can be performed based on the typical 5C architecture: connection, conversion, cyber, cognition, and configuration. This 5-level structure introduced in [5] not only provides a step-by-step guideline for developing CPS applications, but also defines the workflow from the initial data acquisition to the final decision creation [5]–[7].

Among the world-changing applications of CPSs, swarm robotic systems with multiple robots, advanced sensors,

actuators, processing units and networked communication are some of the most important 5C CPS categories [8]. This emerging research area has attracted much attention within recent years because multi-robot CPSs offer many potential advantages, including greater flexibility, collaboration and robustness. With networked communication and robotic sensors/actuators, this kind of swarm robotic CPS has been widely applied successfully to many disciplines for accomplishing complex tasks [9], [10].

In the increasing number of requests of swarm robotic CPSs, collision-free formation control is one of the most important issues and is becoming increasingly crucial [8]–[10]. The purpose of a collision-free coordinated control for a group of robots is to follow a predefined trajectory while maintaining a specified geometrical pattern. This problem has been addressed by several studies that consider the robot's model and graph theory [11]–[13]. However, consensus based control using graph topology has the disadvantage of com-

munication delays in formation control because the flowing links are unidirectional between subsystems. This paper presents an optimal OFA-fuzzy collision-free formation control method for a swarm robotic CPS to avoid the delay problem in consensus formation controllers.

Optimization of fuzzy systems by considering the involved parameters, such as membership functions and rule bases has been one of the most investigated problems. Although there are several studies proposed to cope with this optimization problem [14]–[17], these traditional methods may be trapped at a local optimum in solving multimodal fuzzy optimization problems [17]. Among these approaches, evolutionary fuzzy optimization using metaheuristic algorithms is a new branch for optimizing fuzzy models [18], [19]. Some popular evolutionary fuzzy systems have been developed for improving the behavior of conventional fuzzy systems using a genetic algorithm (GA), particle swarm optimization (PSO) and any colony optimization (ACO) [18]–[21]. However, there has been no attempt to present an orthogonal OFA-fuzzy cyber computing to achieve collision-free formation control of swarm robotic CPSs.

FA developed by Yang [22] is a recent nature-inspired metaheuristic algorithm for global optimization. This swarm intelligence mimics the flashing behavior and attraction characteristics of fireflies in nature [23]. However, the classical FA has the premature convergence issue for solving computationally extensive engineering problems. Although some modified and hybrid FAs have been proposed [23]–[25], these studies neither qualify the FAs using the Taguchi method nor employ a ranking mutation. This paper employs the robust Taguchi method and mutation operation to improve FA searching performance. The proposed orthogonal FA is then applied to develop an OFA-fuzzy paradigm in the cyber level to resolve the collision-free formation control problem of swarm robotic CPSs.

Taguchi method introduced by Genichi Taguchi is a robust statistical approach to optimize the process parameters and improve the quality of manufactured components [26]. Based on successful applications to engineering, marketing and biotechnology, this approach has been applied to design metaheuristic algorithms, including Taguchi based GA, Taguchi based PSO and Taguchi based ACO, by using the signal-to-noise ratio (SNR) and orthogonal array [27]–[29]. On the other hand, mutation is regarded as a major operation to explore decision spaces in evolutionary algorithms. Most algorithms are designed with a fixed mutation probability, thus leading to a local optimum [30], [31]. In this paper, the robust Taguchi method and ranking mutation are fused to design an OFA-fuzzy computing in the cyber level of the proposed swarm robotic CPS. Moreover, the proposed OFA-fuzzy online control scheme is realized in FPGA chips to achieve the collision-free formation control of swarm robotic CPS using SoPC technology. To the authors' best understanding, the research of SoPC-based OFA-fuzzy collision-free formation control for swarm robotic CPSs remains open.

SoPC methodology by means of hardware/software code-sign has contributed to a major revolution in designing modern embedded CPSs consisting of processors and custom logic [32]. Based on the advantages of SoPC, all the hardware circuits and software components can be realized in one FPGA chip. This modern design method not only provides a practical implementation for robotic CPSs, but also improves the system performance, reliability, and cost effectiveness [33]–[35]. The custom hardware modules provide real-time feedback and connection from/to the physical world using sensors/actuators, and the software executed by embedded processors offers programmable cyber sophisticated algorithms in CPS 5C levels. This emerging embedded CPS has attracted much attention due to its potential to greatly accelerate a wide variety of applications.

The rest of this paper is organized as follows. Section 2 introduces a swarm robotic CPS using OFA-fuzzy optimization techniques. Section 3 elucidates the procedure of how to apply the proposed OFA-fuzzy CPS to design a networked swarm robotic CPS to achieve collision-free formation control. Section 4 reports the results of several experiments and comparative works to show the effectiveness and merits of the proposed methods. Section 5 concludes this paper.

II. EVOLUTIONARY SWARM ROBOTIC CPS WITH OFA-FUZZY OPTIMIZATION

A. MODIFIED FIREFLY ALGORITHM

Firefly algorithm is a subfield of computational intelligence motivated by the flashing pattern behavior of fireflies. When applying FA to resolve multiobjective complex optimization problems, an individual is defined as a firefly. The attractiveness of one firefly is proportional to the light intensity seen by adjacent fireflies, which is expressed by

$$\beta(r) = \beta_0 e^{-\gamma r^2} \quad (1)$$

where γ is the absorption coefficient, r is the distance, and β_0 is the attractiveness at $r = 0$.

The distance between any two FA fireflies i at x_i and j at x_j is measured by the following Cartesian distance

$$r_{ij} = \|x_i - x_j\| = \sqrt{\sum_{k=1}^d (x_{i,k} - x_{j,k})^2} \quad (2)$$

where $x_{i,k}$ is the k th component of x_i . The movement of a firefly i attracted to another brighter firefly j is determined by

$$x_i^{t+1} = x_i^t + \beta e^{-\gamma r_{ij}^2} (x_j^t - x_i^t) + \alpha_t \varepsilon_i^t \quad (3)$$

where t is an iteration counter and ε_i^t is a random number vector at t . α_t is given by

$$\alpha_t = \alpha_0 \delta^t, 0 < \delta < 1 \quad (4)$$

where α_0 is an initial scaling parameter and δ is a cooling factor in the FA.

TABLE 1. OFA control parameters and their levels.

	α_0	β_0	γ	δ	P	N_{fa}
Level 1	0.2	0.5	0.3	1	100	100
Level 2	0.5	1.0	0.5	10	200	150
Level 3	1.0	2.0	0.7	20	300	200
Level 4	2.0	3.0	0.9	30	400	250
Level 5	5.0	5.0	1.0	40	500	300

During the FA evolution for searching optimal solutions, mutation is a major process to increase searching diversity and explore decision spaces. This study adopts a rank-based mutation strategy to overcome the limitations of the FA, especially for complex and multidimensional optimization solving. The mutation probability is determined based on the individual’s fitness and its rank in the FA population. This strategy balances the exploration and exploitation of the FA searching space. In the proposed modified FA, the mutation probability of each individual P_i with fitness value $F(i)$ is expressed by

$$P_i = P_{\min} + \frac{\text{rank}(i)}{P} (P_{\max} - P_{\min}) \frac{F_{\text{ave}}}{F(i)} \quad (5)$$

where P is the population size, and $\text{rank}(i)$ is the fitness rank of individual i in the population. P_{\max} and P_{\min} are the maximum and minimum FA mutation probabilities, respectively. F_{ave} denotes the average fitness value.

Parameter setting is an important issue in the design of evolutionary algorithms. In the proposed modified FA, there are six parameters, including γ , β_0 , α_0 , δ , and P as well as the number of generations (N_{fa}). These parameters influence the FA convergence behavior. This study employs the Taguchi method to qualify the FA parameters using the $L_{25}(5^6)$ orthogonal array and small-the-better characteristic SNR. Table 1 lists the control parameters and their levels in the proposed evolutionary OFA computing paradigm.

B. OFA-FUZZY OPTIMIZATION

There are typically four parts in a fuzzy system, including the fuzzifier, knowledge base, fuzzy inference engine and defuzzifier. The fuzzy inference engine employs fuzzy IF-THEN rules to perform a mapping from an input vector $x = [x_1, \dots, x_n]^T \in R^n$ to an output variable $y \in R$. The output y is computed as the weighted average of the rule consequent

$$y = \frac{\sum_{i=1}^K \beta_i(x) y_i}{\sum_{i=1}^K \beta_i(x)} \quad (6)$$

where K denotes the number of rules, y_i is the output variable, and $\beta_i(x)$ is the degree of activation of the i th rule:

$$\beta_i(x) = \prod_{j=1}^n \mu_{A_{ij}}(x_j), \quad i = 1, 2, \dots, K \quad (7)$$

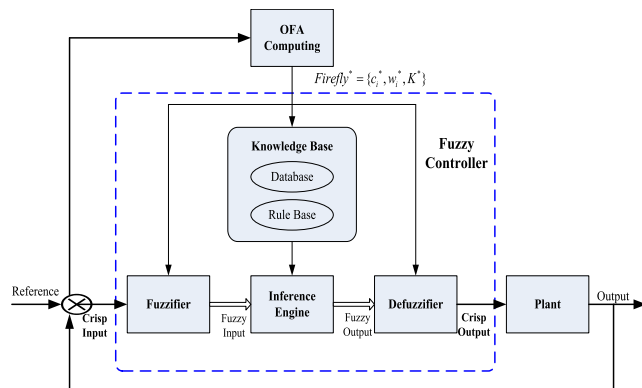


FIGURE 1. Structure of the proposed OFA-fuzzy optimization system.

where $\mu_{A_{ij}}(x_j)$ is the membership function of the fuzzy set A_{ij} in the antecedent of R_i . In the proposed OFA-fuzzy optimization, the membership function of the fuzzy set has a triangular shape with the parameters c_i and w_i , where c_i is the center value of fuzzy sets and w_i is the width. Two adjacent fuzzy sets overlap by half.

Fig. 1 presents the structure of the proposed OFA-fuzzy optimization system. The performance of such a fuzzy system is influenced by the membership functions defined by the center vector c_i , width vector w_i and the number of rules K . To construct an optimal fuzzy structure, this tuning problem is resolved via the OFA to improve the fuzzy performance. Both the number of fuzzy rules and membership functions are considered in this study to evolve an optimal fuzzy system. This OFA-fuzzy optimization outperforms conventional GA, PSO and ACO fuzzy optimization methods by exploiting its strong FA optimization capability.

In the proposed OFA-fuzzy optimization, a firefly is defined by the fuzzy structure parameters, such that $\text{Firefly} = \{c_i, w_i, K\}$. The initial fireflies of the FA population are randomly generated and the optimal fuzzy model $\text{Firefly}^* = \{c_i^*, w_i^*, K^*\}$ is evolved via the biological FA process. Typically, the fitness function using SNR is defined by the mean square error (MSE) with N_T sample to evaluate the candidate solutions:

$$\text{Fitness_SNR} = -10 \log \left(\frac{1}{N_T} \sum_{k=1}^{N_T} (y_p^*(k) - y_p(k))^2 \right) \quad (8)$$

where $y_p(k)$ is the output in the k th sampling data and $y_p^*(k)$ is the predicted output.

C. OFA-FUZZY BASED SWARM ROBOTIC CPS

Fig. 2 presents the realization of the proposed OFA-fuzzy based swarm robotic CPS to achieve distributed formation control using the 5C structure and leader-follower strategy. All the robots communicate with each other via the wireless network. Having the advantages of distributed control approach, each mobile robot is implemented using an independent 5C architecture. This study includes the

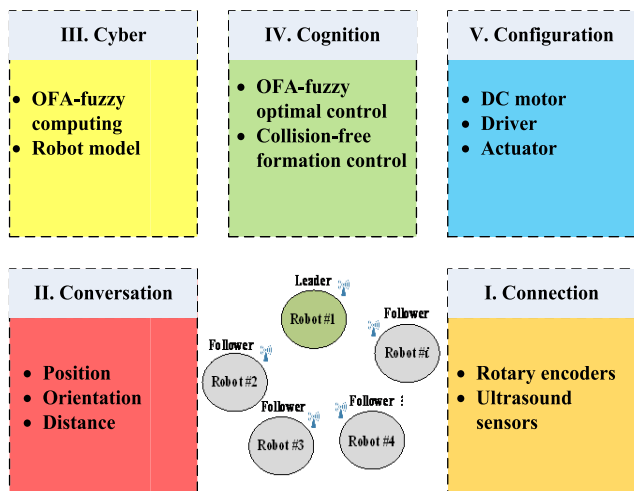


FIGURE 2. Realization of the OFA-fuzzy based swarm robotic CPS.

four-wheeled redundant mobile robots with Swedish wheels to construct the swarm robotic CPS.

As shown in Fig. 2, the advanced sensors such as rotary encoders and ultrasound sensors are considered in smart connection level to ensure real-time data acquisition from the robotic physical world. The data-to-information conversion level receives the sensed raw data and then converts it to useful information, including position, orientation and distance. With the important information from the leader robot and follower robots, the cyber level performs intelligent analytics by means of OFA-fuzzy computing and vehicle model. The cognition level incorporates with the cyber level to make decisions, and aims to achieve OFA-fuzzy optimal control. Finally, the configuration level of each robot drives the DC motors mounted on the omnidirectional wheels to perform leader-follower collision-free formation control.

III. COLLISION-FREE OFA-FUZZY FORMATION CONTROL
A. MATHEMATICAL MODELING AND MOTION CONTROL

Fig. 3 depicts the geometry of the four-wheeled Swedish mobile robots in the proposed swarm robotic CPS with 5C levels. In the cyber level of robot modeling, the mathematical model of the four-wheeled mobile robot is described by

$$\begin{bmatrix} v_1(t) \\ v_2(t) \\ v_3(t) \\ v_4(t) \end{bmatrix} = \begin{bmatrix} r\omega_1(t) \\ r\omega_2(t) \\ r\omega_3(t) \\ r\omega_4(t) \end{bmatrix} = P(\theta(t)) \begin{bmatrix} \dot{x}(t) \\ \dot{y}(t) \\ \dot{\theta}(t) \end{bmatrix}, \quad (9)$$

$$P(\theta(t)) = \begin{bmatrix} -\sin(\delta + \theta) & \cos(\delta + \theta) & L \\ -\cos(\delta + \theta) & -\sin(\delta + \theta) & L \\ \sin(\delta + \theta) & -\cos(\delta + \theta) & L \\ \cos(\delta + \theta) & \sin(\delta + \theta) & L \end{bmatrix}$$

where δ is $\pi/4$; r denotes the radius of the driving wheel; L represents the distance from the wheel’s center to the geometric center of the Swedish mobile robot; $v_i(t)$ and $\omega_i(t)$, $i = 1, 2, 3, 4$ denote the linear and angular velocities of each

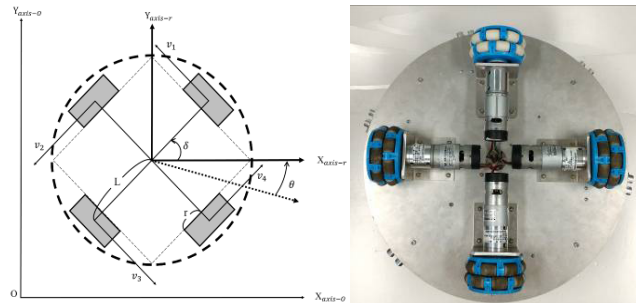


FIGURE 3. Geometry of the four-wheeled Swedish mobile robot.

omnidirectional wheel; and $[x(t)y(t)\theta(t)]^T$ is the pose of the redundant omnidirectional mobile robot.

In robotics research, robots with four degrees-of-freedom (DOF) are categorized as redundant robots because the number of DOF in the moving frame is three. To derive the inverse kinematics of the mobile robots, it is required to obtain the inverse matrix of $P(\theta(t))$. Although the transformation matrix $P(\theta(t))$ in (9) is singular for any θ in this redundant omnidirectional mobile robot system, its left pseudo-inverse matrix $P^\#(\theta(t))$ can be determined by means of $P^\#(\theta(t))P(\theta(t)) = I$, expressed by

$$P^\#(\theta(t)) = \begin{bmatrix} \frac{-\sin(\delta + \theta)}{\cos^2(\delta + \theta)} & \frac{-\cos(\delta + \theta)}{-\sin^2(\delta + \theta)} & \frac{\sin(\delta + \theta)}{-\cos^2(\delta + \theta)} & \frac{\cos(\delta + \theta)}{\sin^2(\delta + \theta)} \\ \frac{1}{4L} & \frac{1}{4L} & \frac{1}{4L} & \frac{1}{4L} \end{bmatrix} \quad (10)$$

The pseudo-inverse matrix approach copes with the redundant inverse kinematic problem of the four-wheeled mobile robots. Combining (9) and (10), the following inverse kinematics of the redundant robots in multi-robot CPS is obtained

$$\begin{bmatrix} \dot{x}(t) \\ \dot{y}(t) \\ \dot{\theta}(t) \end{bmatrix} = P^\#(\theta(t)) \begin{bmatrix} v_1(t) \\ v_2(t) \\ v_3(t) \\ v_4(t) \end{bmatrix} \quad (11)$$

This inverse kinematic model is practical for designing a motion controller in the cognition level of each robot CPS using the proposed OFA-fuzzy computational intelligence.

With the derived inverse kinematics model of mobile robots, the next goal is to develop a motion controller and prove its stability. By doing so, one defines the current pose of the mobile robot $Y = [x(t) y(t) \theta(t)]^T$ and the desired trajectory of the mobile robot $Y_d = [x_d(t) y_d(t) \theta_d(t)]^T$. Hence, the tracking error vector of the four-wheeled omnidirectional mobile robot is expressed by

$$Y_e = \begin{bmatrix} x_e(t) \\ y_e(t) \\ \theta_e(t) \end{bmatrix} = \begin{bmatrix} x(t) \\ y(t) \\ \theta(t) \end{bmatrix} - \begin{bmatrix} x_d(t) \\ y_d(t) \\ \theta_d(t) \end{bmatrix} = Y - Y_d \quad (12)$$

which gives

$$\begin{aligned} \dot{Y}_e &= \begin{bmatrix} \dot{x}_e(t) \\ \dot{y}_e(t) \\ \dot{\theta}_e(t) \end{bmatrix} = \begin{bmatrix} \dot{x}(t) \\ \dot{y}(t) \\ \dot{\theta}(t) \end{bmatrix} - \begin{bmatrix} \dot{x}_d(t) \\ \dot{y}_d(t) \\ \dot{\theta}_d(t) \end{bmatrix} \\ &= P^\#(\theta(t)) \begin{bmatrix} r\omega_1(t) \\ r\omega_2(t) \\ r\omega_3(t) \\ r\omega_4(t) \end{bmatrix} - \begin{bmatrix} \dot{x}_d(t) \\ \dot{y}_d(t) \\ \dot{\theta}_d(t) \end{bmatrix} \end{aligned} \quad (13)$$

Obviously, the control goal is to find the controlled angular velocity vector $[\omega_1(t) \ \omega_2(t) \ \omega_3(t) \ \omega_4(t)]^T$ to track the differentiable trajectory $[x_d(t) \ y_d(t) \ \theta_d(t)]^T$, such that the closed-loop error system is globally asymptotically stable. In this paper, the following redundant control law is proposed to achieve motion control

$$\begin{aligned} \begin{bmatrix} v_1(t) \\ v_2(t) \\ v_3(t) \\ v_4(t) \end{bmatrix} &= P(\theta(t)) \left(-K_P \begin{bmatrix} x_e(t) \\ y_e(t) \\ \theta_e(t) \end{bmatrix} - K_I \begin{bmatrix} \int_0^t x_e(\tau) d\tau \\ \int_0^t y_e(\tau) d\tau \\ \int_0^t \theta_e(\tau) d\tau \end{bmatrix} \right. \\ &\quad \left. - K_D \begin{bmatrix} \dot{x}_e(t) \\ \dot{y}_e(t) \\ \dot{\theta}_e(t) \end{bmatrix} + \begin{bmatrix} \dot{x}_d(t) \\ \dot{y}_d(t) \\ \dot{\theta}_d(t) \end{bmatrix} \right) \end{aligned} \quad (14)$$

where the control matrices are diagonal and positive, meanly that $K_P = \text{diag}[k_{xp}k_{yp}k_{\theta p}]$, $K_I = \text{diag}[k_{xi}k_{yi}k_{\theta i}]$, and $K_D = \text{diag}[k_{xd}k_{yd}k_{\theta d}]$. Substituting (14) into (13) leads to the closed-loop error system

$$\begin{aligned} \dot{Y}_e &= \begin{bmatrix} \dot{x}_e(t) \\ \dot{y}_e(t) \\ \dot{\theta}_e(t) \end{bmatrix} = \left(-K_P \begin{bmatrix} x_e(t) \\ y_e(t) \\ \theta_e(t) \end{bmatrix} \right. \\ &\quad \left. - K_I \begin{bmatrix} \int_0^t x_e(\tau) d\tau \\ \int_0^t y_e(\tau) d\tau \\ \int_0^t \theta_e(\tau) d\tau \end{bmatrix} - K_D \begin{bmatrix} \dot{x}_e(t) \\ \dot{y}_e(t) \\ \dot{\theta}_e(t) \end{bmatrix} \right) \end{aligned} \quad (15)$$

The asymptotical stability of the closed-loop error system is proven by selecting the Lyapunov function

$$\begin{aligned} V(t) &= \frac{1}{2} [x_e(t) \ y_e(t) \ \theta_e(t)] \begin{bmatrix} x_e(t) \\ y_e(t) \\ \theta_e(t) \end{bmatrix} \\ &\quad + \frac{1}{2} \left[\int_0^t x_e(\tau) d\tau \ \int_0^t y_e(\tau) d\tau \ \int_0^t \theta_e(\tau) d\tau \right] K_I \\ &\quad \times \begin{bmatrix} \int_0^t x_e(\tau) d\tau \\ \int_0^t y_e(\tau) d\tau \\ \int_0^t \theta_e(\tau) d\tau \end{bmatrix} + \frac{1}{2} [x_e(t) \ y_e(t) \ \theta_e(t)] K_D \\ &\quad \times \begin{bmatrix} x_e(t) \\ y_e(t) \\ \theta_e(t) \end{bmatrix} > 0 \end{aligned}$$

and its time derivative is

$$\dot{V}(t) = - [x_e(t) \ y_e(t) \ \theta_e(t)] K_P \begin{bmatrix} x_e(t) \\ y_e(t) \\ \theta_e(t) \end{bmatrix} < 0$$

which shows that \dot{V} is negative definite, and Barbalat's lemma implies that Y_e approaches zero as time tends to infinity.

TABLE 2. Fuzzy rule base of the OFA-fuzzy redundant controller.

$\Delta K \backslash e$	NB	NM	NS	ZO	PS	PM	PB
NB	PB	PB	PB	PB	PS	ZO	NS
NM	PB	PB	PM	PM	ZO	NS	NM
NS	PB	PM	PM	PS	NS	NM	NB
ZO	ZO	ZO	ZO	ZO	ZO	ZO	ZO
PS	NB	NM	NS	PS	PM	PM	PB
PM	NM	NS	ZO	PM	PB	PB	PB
PB	NS	ZO	PS	PB	PB	PB	PB

The globally asymptotical stability of the closed-loop error system is therefore ensured, meaning that $Y \rightarrow Y_d$ as $t \rightarrow \infty$. This result indicates that the proposed motion controller is capable of steering the four-wheeled omnidirectional robot to follow any differentiable and time-varying trajectory.

B. OFA-FUZZY ONLINE CONTROL

In the cognition level, an OFA-optimized fuzzy controller is developed to online adjust the parameters $K_P = \text{diag}[k_{xp}k_{yp}k_{\theta p}]$, $K_I = \text{diag}[k_{xi}k_{yi}k_{\theta i}]$ and $K_D = \text{diag}[k_{xd}k_{yd}k_{\theta d}]$. The control matrices in (14) are online adjusted at every sampling to achieve motion control in each mobile robot CPS. This OFA online tuning method is superior to conventional offline and hand-tuning approaches.

Considering the position and orientation errors of the OFA-fuzzy multi-robot CPS with n robots, the objective function (performance index) using SNR is defined by

$$\text{Fitness_SNR} = -10 \log \left[w_e \left(\sum_{i=1}^n |x_{ei}| + |y_{ei}| + |\theta_{ei}| \right) + w_r \sum_{i=1}^n N_i \right] \quad (16)$$

where (x_{ei}, y_{ei}) and θ_{ei} are the position and orientation errors of the i th robot, respectively, and N_i is the number of rule bases of the i th robot. Once the optimal fuzzy model $\text{Firefly}^* = \{c_i^*, w_i^*, K^*\}$ is obtained via the proposed OFA computing, this fuzzy optimization in the cyber level is utilized to develop an OFA-fuzzy optimal controller in the cognition level to accomplish formation control. The redundant controller in the cognition level of each robot CPS online tunes the control matrices K_P, K_I, K_D by using the fuzzy rule bases. Table 2 lists the fuzzy rule base of the proposed OFA-fuzzy robust motion controller in the cognition level of the proposed swarm robotic CPS. The linguistic statements NB (Negative Big), NM (Negative Medium), NS (Negative Small), ZO (Zero), PS (Positive Small), PM (Positive Medium) and PB (Positive Big) are included to describe the fuzzy rule base.

C. LEADER-FOLLOWER DISTRIBUTED FORMATION CONTROL

Fig. 4 depicts the broadcast leader-follower formation control of the swarm robotic CPS with three robots. The leader robot moves along a predefined trajectory and the follower robots

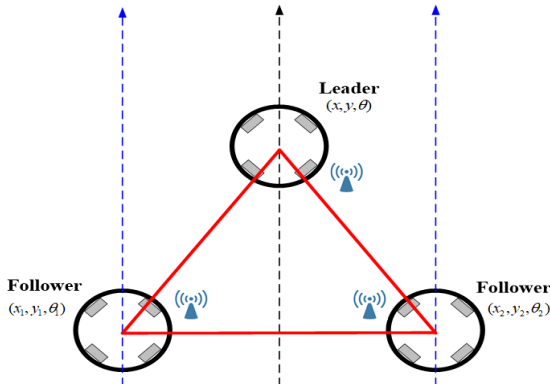


FIGURE 4. Broadcast leader-follower formation control.

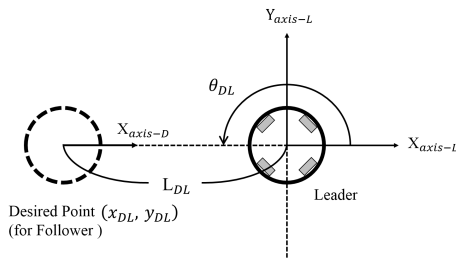


FIGURE 5. Relationship of the leader and follower robots.

maintain the desired formation with respect to the leader robot. All the robot CPSs are independently steered by using the control scheme in (14), and the control parameters are online tuned by means of the OFA-fuzzy paradigm. Note that each mobile robot is equipped with an independent robotic CPS in Fig. 2 to perform distributed formation control.

In the proposed leader-follower swarm robotic CPS, it is very important to derive the relationship between the leader robot and follower robot. As shown in Fig. 5, the geometrical relationship is described by

$$\begin{aligned} x_{DL} &= L_{DL} \cdot \cos(\theta_{DL}) \\ y_{DL} &= L_{DL} \cdot \sin(\theta_{DL}) \end{aligned} \quad (17)$$

where $(x_{DL}, y_{DL}, \theta_{DL})$ is the desired position and orientation of the follower robot in formation control, and L_{DL} is the distance between the leader and follower in formation control. Furthermore, based on the coordinates of follower robot in Fig. 6, one obtains the relationships:

$$\begin{aligned} x_{LF} &= L_{LF} \cdot \cos(\theta_{LF}) \\ y_{LF} &= L_{LF} \cdot \sin(\theta_{LF}) \end{aligned} \quad (18)$$

$$\begin{aligned} x_{DF} &= x_{DL} \cdot \cos(\varphi) + y_{DL} \cdot \sin(\varphi) + x_{LF} \\ y_{DF} &= -x_{DL} \cdot \sin(\varphi) + y_{DL} \cdot \cos(\varphi) + y_{LF} \end{aligned} \quad (19)$$

where (x_{DF}, y_{DF}) is the desired position of the follower robot, L_{LF} is the distance between the leader and follower, (x_{LF}, y_{LF}) is the position of the leader robot based on the coordinates of the follower robot, θ_{LF} is the orientation of follower robot with respect to L_{LF} and $\varphi = \theta_{FO} - \theta_{LO}$ is

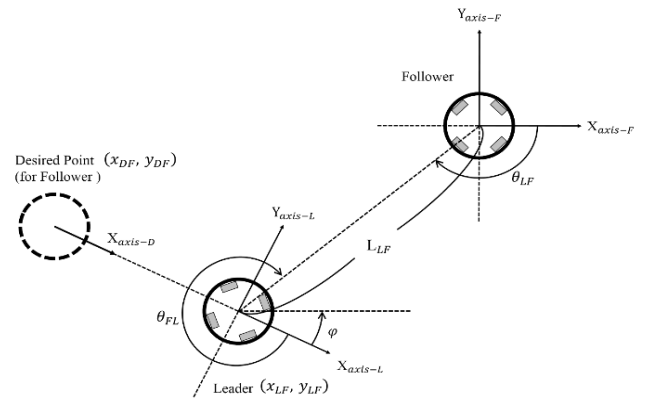


FIGURE 6. Geometry of the leader-follower swarm robotic CPS.

the orientation of the follower robot with respect to the leader robot. Moreover, it is easy to obtain the following relationship in world coordinates:

$$\begin{aligned} \theta_{mF} &= \tan^{-1} \left(\frac{x_{LO} - x_{FO}}{y_{LO} - y_{FO}} \right) \\ \theta_{mL} &= \tan^{-1} \left(\frac{x_{FO} - x_{LO}}{y_{FO} - y_{LO}} \right) \\ \theta_{LF} &= \theta_{mF} - \theta_{FO} \\ \theta_{FL} &= \theta_{mL} - \theta_{LO} \end{aligned} \quad (20)$$

where (x_{FO}, y_{FO}) is the position of the follower robot in world coordinates, (x_{LO}, y_{LO}) is the position of the leader robot in world coordinates, θ_{FO} and θ_{LO} are the orientations of the follower robot and leader robot with respect to world coordinates, respectively. θ_{FL} is the orientation of leader robot with respect to L_{LF} , θ_{mL} is the orientation of leader robot with respect to the follower robot in world coordinates, and θ_{mF} is the orientation of the follower robot with respect to leader robot in world coordinates. The relationship of the orientations φ , θ_{LF} and θ_{FL} is obtained as follows:

$$\begin{aligned} \varphi &= \theta_{mF} - \theta_{LF} + \theta_{FL} - \theta_{mL} \\ &= \pi - \theta_{LF} + \theta_{FL} \end{aligned} \quad (21)$$

Note that the orientation and distance are measured by sensors in the connection level and are converted into useful information in the data-to-information level to perform formation control.

D. OBSTACLE AVOIDANCE USING ARTIFICIAL POTENTIAL FIELD (APF)

Artificial potential field methods are rapidly gaining popularity in obstacle avoidance applications for swarm robotic CPSs. In this study, this methodology is combined with the OFA-fuzzy control scheme to achieve collision-free formation control in the configuration space. Considering a swarm robotic CPS with n robots and M obstacles, the repulsive field U of robot i is expressed by

$$U(q_i) = U_1(q_i) + U_2(q_i) \quad (22)$$

where q_i is the configuration of robot i , U_1 is the repulsive potential from other robots and U_2 is the repulsive potential from obstacles, defined by

$$U_1(q_i) = \begin{cases} \frac{1}{2}\varsigma_1 \left(\sum_{i=1, i \neq j}^n \left(\frac{1}{\rho(q_{ij})} - \frac{1}{\rho_0} \right)^2 \right), & \text{if } \rho(q_{ij}) \leq \rho_0 \\ 0, & \text{if } \rho(q_{ij}) > \rho_0 \end{cases}$$

$$U_2(q_i) = \begin{cases} \frac{1}{2}\varsigma_2 \left(\sum_{k=1}^M \left(\frac{1}{\rho(q_{ik})} - \frac{1}{\rho_0} \right)^2 \right), & \text{if } \rho(q_{ik}) \leq \rho_0 \\ 0, & \text{if } \rho(q_{ik}) > \rho_0 \end{cases} \quad (23)$$

where ς_1 and ς_2 are scalar gains that determine the influence of the repulsive field, $\rho(q_{ij}) = \|q_i - q_j\|_2$ is the Euclidean distance between q_i and q_j . $q_{k,obstacle}$ is the configuration of the k th obstacle and $\rho(q_{ik}) = \|q_i - q_{k,obstacle}\|_2$ is the distance between q_i and $q_{k,obstacle}$. ρ_0 is the distance of influence of an obstacle.

The corresponding repulsive force is given by the negative gradient of the repulsive field,

$$F_{i,rep}(q_i) = -\nabla U(q_i) = F_{i,rep1}(q_i) + F_{i,rep2}(q_i) \quad (24)$$

where

$$F_{i,rep1}(q_i) = \begin{cases} \varsigma_1 \sum_{i=1, i \neq j}^n \left(\frac{1}{\rho(q_{ij})} - \frac{1}{\rho_0} \right) \frac{1}{\rho^2(q_{ij})} \frac{q_i - q_j}{\rho(q_{ij})}, & \text{if } \rho(q_{ij}) \leq \rho_0 \\ 0, & \text{if } \rho(q_{ij}) > \rho_0 \end{cases}$$

$$F_{i,rep2}(q_i) = \begin{cases} \varsigma_2 \sum_{k=1}^M \left(\frac{1}{\rho(q_{ik})} - \frac{1}{\rho_0} \right) \frac{1}{\rho^2(q_{ik})} \frac{q_i - q_{k,obstacle}}{\rho(q_{ik})}, & \text{if } \rho(q_{ik}) \leq \rho_0 \\ 0, & \text{if } \rho(q_{ik}) > \rho_0 \end{cases} \quad (25)$$

where $F_{i,rep1}(q_i)$ and $F_{i,rep2}(q_i)$ are the repulsive forces of the i th robot due to other robots and obstacles in the configuration space, respectively. The ultrasound sensors are mounted on each mobile robot to detect the distance between the robot and obstacles in CPS Level 1. These signals are then converted to useful distance and APF force information using the embedded CPU in CPS Level 2. With the formation control scheme (14) and APF (22), the proposed OFA-fuzzy motion controller in Level 4 determines the optimal commands to steer the mobile robots to achieve collision-free formation control.

E. SoPC REALIZATION

This subsection aims to implement the proposed networked swarm robotic CPS in FPGAs using SoPC technology. Fig. 7 presents the structure of the distributed leader-follower swarm robotic CPS. In this distributed computing system,

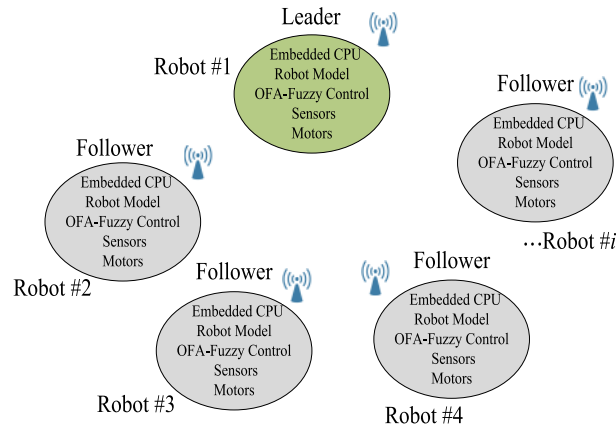


FIGURE 7. Structure of the distributed swarm robotic CPS.

each mobile robot has an independent CPS and is implemented in one FPGA chip. All the robotic CPS 5C levels are integrated into one chip to provide close interaction between cyber and physical worlds.

As shown in Fig. 7, each robotic CPS is a specialized embedded system under real-time conditions. The embedded CPUs act as central units in the 2nd conversion level, 3rd cyber level and 4th cognition level to perform sophisticated algorithms in cyber space, including OFA-fuzzy optimization, robot modeling and redundant control. The CPS 1st connection and 5th configuration levels bridge the physical and cyber worlds, and they are realized by Verilog hardware description language (HDL) and synthesized in the same FPGA. This hardware/software codesign methodology offers flexible software design and high-performance hardware design in one chip.

This study utilizes an inexpensive DE1-SOC development kit to implement the mobile robot CPS. This FPGA kit presents a robust hardware design platform built around the Altera system-on-chip (SoC) FPGA, which combines the latest dual-core Cortex-A9 embedded cores with industry-leading programmable logic for ultimate design flexibility. The hard-core processor (hard processor system, HPS) is integrated into each mobile robot CPS to perform complex computing in the cyber, cognition and configuration levels. The advanced microcontroller bus architecture advanced extensible interface bridge (AMBA AXI) interfaces tied seamlessly with the peripherals and memory.

Fig. 8 presents the FPGA realization of each mobile robot CPS in the proposed OFA-fuzzy swarm robotic CPS. The Verilog HDL based robotic hardware IPs have been developed to interface with the cyber and physical worlds, such as digital filters, QEP (Quadrature Encoder Pulse), PWM (Pulse Width Modulation) and ultrasound modules. The QEP and ultrasound modules convert the received signals from rotary encoders and sonar sensors to perform data-to-information conversion. The PWM module serves as the CPS 5th configuration level, and receives the output decisions made by the cyber world computing to steer mobile robots in the physical

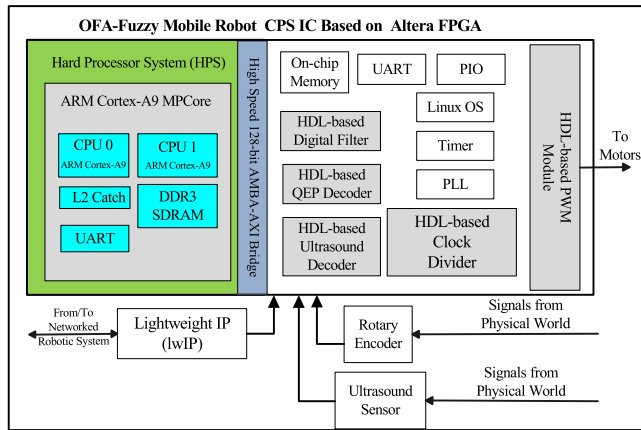


FIGURE 8. FPGA implementation of each mobile robot CPS.

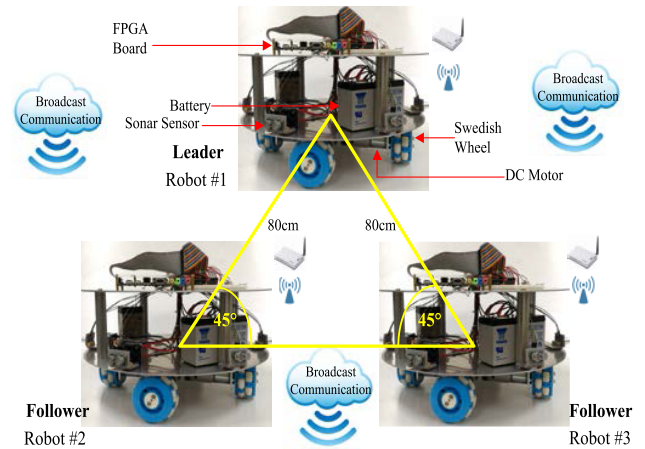


FIGURE 9. Architecture of the OFA-fuzzy multi-robot CPS.

world to achieve distributed adaptive formation control. The phase locked loop (PLL) and clock divider IPs are used to provide different clock frequency sources in the mobile robot CPS. The networking lightweight IP (lwIP) and embedded Linux OS are integrated in the same Altera FPGA chip to achieve broadcast networked communication.

IV. EXPERIMENTAL RESULTS, COMPARATIVE WORKS AND DISCUSSION

A. ARCHITECTURE of the SWARM ROBOTIC CPS SYSTEM

Fig. 9 presents the architecture of the FPGA-based hybrid OFA-fuzzy swarm robotic CPS used to examine the effectiveness of the proposed methods. There are three four-wheeled omnidirectional mobile robots with Swedish wheels in the leader-follower multi-robot CPS architecture, including one leader-robot and two follower robots with the parameters: $L = 0.25\text{m}$, $r = 0.0508\text{m}$. In the proposed SoPC-based swarm robotic CPS, each robot is equipped with a battery, an FPGA development kit, DC motors, sonar sensors and Swedish wheels under wireless networked communication. This embedded realization using hardware/software codesign provides a cost-effective hybrid OFA-fuzzy optimization for designing swarm robotic CPSs.

B. FORMATION CONTROL WITH OBSTACLE AVOIDANCE

The following experiment was conducted to verify the effectiveness of the proposed OFA-fuzzy distributed formation control with obstacle avoidance. Fig. 10 depicts the experimental setup of the formation control. The desired circular trajectory is expressed by $[x_d(t) \ y_d(t) \ \theta_d(t)]^T = [1.5 \cos(\omega_i t)\text{m} \ 1.5 \sin(\omega_i t)\text{m} \ \pi/2 \text{rad}]^T$, $\omega_i = 0.35\text{rad/sec}$. for the leader robot, and an obstacle is placed in the working space. The two follower robots aim to maintain the triangular formation while the leader robot tracks the desired trajectory.

Fig. 11 presents the experimental results of OFA-fuzzy collision-free formation control. The three mobile robots are initially set at different poses. The leader robot in the swarm robotic CPS tracks the collision-free path and the two

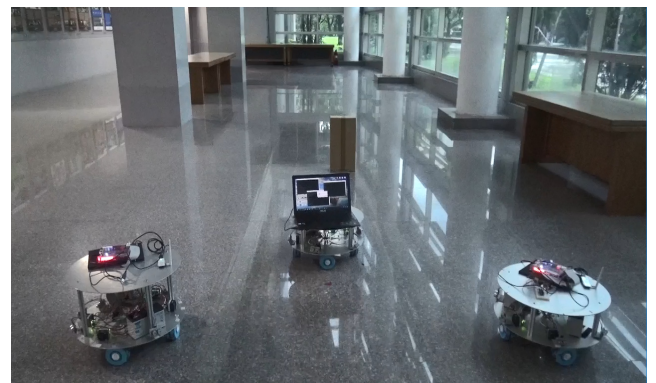


FIGURE 10. Experimental setup for the OFA-fuzzy distributed formation control.

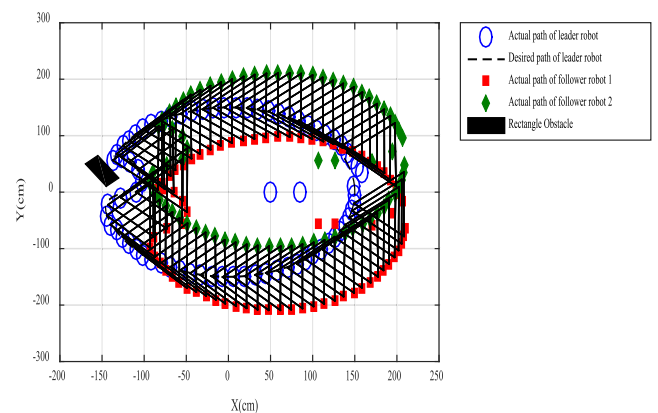


FIGURE 11. Experimental results of OFA-fuzzy formation control.

followers maintain the triangular formation. The tracking error of leader robot is depicted in Fig. 12. The formation errors of the swarm robotic CPS are presented in Fig. 13. The two follower robots maintain the shape while the leader robot avoids the obstacle. These experimental results demonstrate that the proposed FPGA-based hybrid OFA-fuzzy

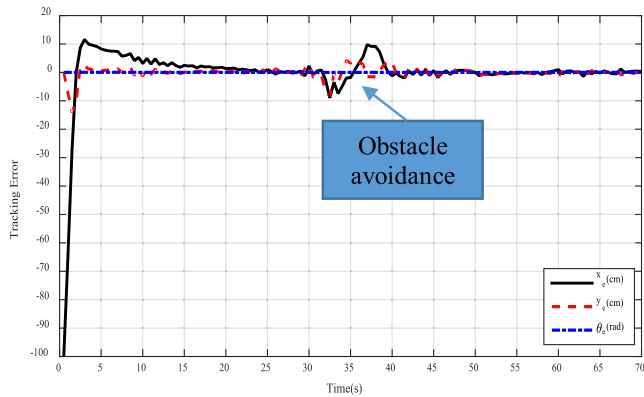


FIGURE 12. Tracking error of the leader robot in the multi-robot CPS.

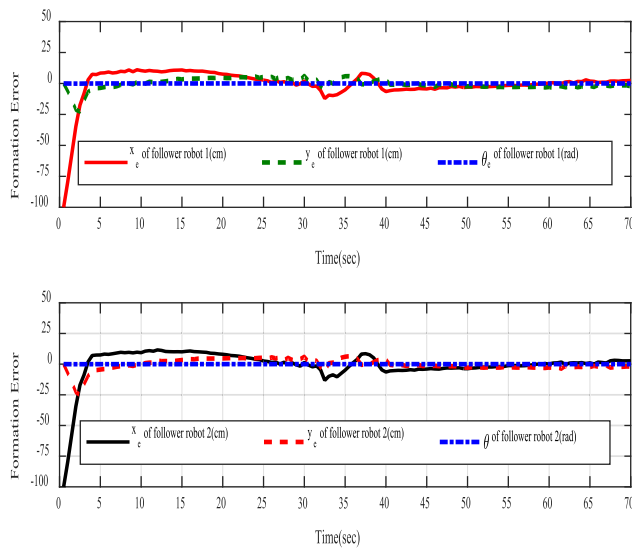


FIGURE 13. Formation errors of the follower robots.

optimization is capable of accomplishing collision-free formation control via the 5C levels of swarm robotic CPSs.

C. COMPARATIVE WORKS

The comparative works are utilized to present the merits of the proposed OFA-fuzzy metaheuristics over other conventional methods in designing formation controller of swarm robotic CPSs. Compared with the offline computing, the proposed OFA-fuzzy optimization in the cognition level of multi-robot CPSs reveals the advantage of real-time online tuning. In particular, this study adapts SoPC technology to implement such an intelligent robotic system, thus presenting an inexpensive distributed swarm robotic CPS. Furthermore, the broadcast networked communication strategy circumvents the difficulty of the delay problem in conventional consensus formation control of multi-robot CPS.

Moreover, in order to demonstrate the superiority of the proposed cyber OFA-fuzzy computing over conventional evolutionary methods in designing multi-robot CPSs, this approach has been compared with the performance of GA-fuzzy and PSO-fuzzy paradigms for the same task. Fig. 14 compares the performance for achieving collision-free formation control using GA-fuzzy, PSO-fuzzy and

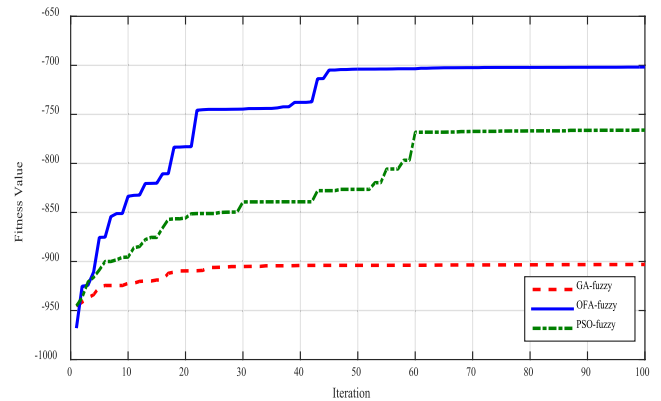


FIGURE 14. Comparative work of the OFA-fuzzy optimization and conventional methods to achieve collision-free formation control.

OFA-fuzzy computing methods with the same fitness function in (16). Fig. 14 shows that the proposed cyber OFA-fuzzy optimization is superior to the GA-fuzzy and PSO-fuzzy approaches because it converges to the optimum more quickly and avoids the premature convergence. Through these experimental results and comparative works, the proposed hybrid metaheuristic OFA-fuzzy optimization outperforms the conventional methods for designing swarm robotic CPS to achieve collision-free formation control.

V. CONCLUSION

This paper has presented a collision-free fuzzy formation control method of swarm robotic CPSs using the robust OFA computing. The bio-inspired OFA-fuzzy computing is utilized to develop optimal cyber and cognition levels in swarm robotic CPS 5C architecture. With the physical signals from/to robotic sensors/actuators, the OFA-fuzzy based cyber and cognition levels are incorporated with smart connection, data-to-information conversion and configuration levels to design a pragmatic multi-robot CPS using SoPC technology. The proposed broadcast robotic CPS avoids the communication delay in conventional consensus multi-robot CPSs under a directed network topology. Experimental results and comparative works demonstrate the merits of the proposed FPGA-based OFA-fuzzy swarm robotic CPS to achieve distributed collision-free formation control.

REFERENCES

- [1] M. Rungger and P. Tabuada, "A notion of robustness for cyber-physical systems," *IEEE Trans. Autom. Control*, vol. 61, no. 8, pp. 2108–2123, Aug. 2016.
- [2] S. Wen and G. Guo, "Control and resource allocation of cyber-physical systems," *IET Control Theory Appl.*, vol. 10, no. 16, pp. 2038–2048, 2016.
- [3] Y. Guo, X. Hu, B. Hu, J. Cheng, M. Zhou, and R. Y. K. Kwok, "Mobile cyber physical systems: Current challenges and future networking applications," *IEEE Access*, vol. 16, pp. 12360–12368, 2018.
- [4] K. M. Alam and A. E. Saddik, "A digital twin architecture reference model for the cloud-based cyber-physical systems," *IEEE Access*, vol. 5, pp. 2050–2062, Jan. 2017.
- [5] J. Lee, B. Bagheri, and H.-A. Kao, "A cyber-physical systems architecture for industry 4.0-based manufacturing systems," *Manuf. Lett.*, vol. 3, pp. 18–23, Jan. 2015.
- [6] M. Z. A. Bhuiyan, J. Wu, G. Wang, and G. Cao, "Sensing and decision making in cyber-physical systems: The case of structural event monitoring," *IEEE Trans. Ind. Informat.*, vol. 12, no. 6, pp. 2103–2114, Dec. 2016.

- [7] F. Pasqualetti and Q. Zhu, "Design and operation of secure cyber-physical systems," *IEEE Embedded Syst. Lett.*, vol. 7, no. 1, pp. 3–6, Mar. 2015.
- [8] M. U. Khan, S. Li, Q. Wang, and Z. Shao, "CPS oriented control design for networked surveillance robots with multiple physical constraints," *IEEE Trans. Comput.-Aided Design Integr. Circuits Syst.*, vol. 35, no. 5, pp. 778–791, May 2016.
- [9] Y. Kantaros and M. M. Zavlanos, "Global planning for multi-robot communication networks in complex environments," *IEEE Trans. Robot.*, vol. 32, no. 5, pp. 1045–1061, Oct. 2016.
- [10] A. Adler, M. de Berg, D. Halperin, and K. Solovey, "Efficient multi-robot motion planning for unlabeled discs in simple polygons," *IEEE Trans. Autom. Sci. Eng.*, vol. 12, no. 4, pp. 1309–1317, Oct. 2015.
- [11] Z. Liu, W. Chen, J. Lu, H. Wang, and J. Wang, "Formation control of mobile robots using distributed controller with sampled-data and communication delays," *IEEE Trans. Control Syst. Technol.*, vol. 24, no. 6, pp. 2125–2132, Nov. 2016.
- [12] Z. Meng, W. Ren, Y. Cao, and Z. You, "Leaderless and leader-following consensus with communication and input delays under a directed network topology," *IEEE Trans. Syst., Man, Cybern. B, Cybern.*, vol. 41, no. 1, pp. 75–88, Feb. 2011.
- [13] R. Wang, X. Dong, Q. Li, and Z. Ren, "Distributed adaptive formation control for linear swarm systems with time-varying formation and switching topologies," *IEEE Access*, vol. 4, pp. 8995–9004, 2016.
- [14] Y.-W. Liang, C.-C. Chen, and S. S.-D. Xu, "Study of reliable design using T-S fuzzy modeling and integral sliding mode control schemes," *Int. J. Fuzzy Syst.*, vol. 15, no. 2, pp. 233–243, 2013.
- [15] Y.-C. Hsueh, S.-F. Su, and M.-C. Chen, "Decomposed fuzzy systems and their application in direct adaptive fuzzy control," *IEEE Trans. Cybern.*, vol. 44, no. 10, pp. 1772–1783, Oct. 2014.
- [16] H. K. Lam, "A review on stability analysis of continuous-time fuzzy-model-based control systems: From membership-function-independent to membership-function-dependent analysis," *Eng. Appl. Artif. Intell.*, vol. 67, pp. 390–408, Jan. 2018.
- [17] H. Shen, F. Li, H. Yan, and H. R. Karimi, "Finite-time event-triggered H_∞ control for T-S fuzzy Markov jump systems," *IEEE Trans. Fuzzy Syst.*, vol. 26, no. 5, pp. 3122–3135, Oct. 2018.
- [18] M. Goharimanesh, A. Lashkaripour, S. Shariatnia, and A. A. Akbari, "Diabetic control using genetic fuzzy-PI controller," *Int. J. Fuzzy Syst.*, vol. 16, no. 2, pp. 133–138, 2014.
- [19] J.-S. Lee and C.-L. Teng, "An enhanced hierarchical clustering approach for mobile sensor networks using fuzzy inference systems," *IEEE Internet Things J.*, vol. 4, no. 4, pp. 1095–1103, Aug. 2017.
- [20] C.-F. Juang, T.-L. Jeng, and Y.-C. Chang, "An interpretable fuzzy system learned through online rule generation and multiobjective ACO with a mobile robot control application," *IEEE Trans. Cybern.*, vol. 46, no. 12, pp. 2706–2718, Dec. 2016.
- [21] S.-H. Tsai and Y.-W. Chen, "A novel fuzzy identification method based on ant colony optimization algorithm," *IEEE Access*, vol. 4, pp. 3747–3756, 2016.
- [22] X.-S. Yang, "Firefly algorithm, stochastic test functions and design optimisation," *Int. J. Bio-Inspired Comput.*, vol. 2, no. 2, pp. 78–84, 2010.
- [23] A. R. Cukla, R. C. Izquierdo, F. A. P. Borges, E. A. Perondi, and F. J. Lorini, "Optimum cascade control tuning of a hydraulic actuator based on firefly metaheuristic algorithm," *IEEE Latin Amer. Trans.*, vol. 16, no. 2, pp. 384–390, Feb. 2018.
- [24] A. Mishra, V. N. K. Gundavarapu, V. R. Bathina, and D. C. Duvvada, "Real power performance index and line stability index-based management of contingency using firefly algorithm," *IET Gener., Transmiss. Distrib.*, vol. 10, no. 10, pp. 2327–2335, 2016.
- [25] H. Su, Y. Cai, and Q. Du, "Firefly-algorithm-inspired framework with band selection and extreme learning machine for hyperspectral image classification," *IEEE J. Sel. Topics Appl. Earth Observ. Remote Sens.*, vol. 10, no. 1, pp. 309–320, Jan. 2017.
- [26] G. Taguchi, *Introduction to Quality Engineering: Designing Quality Into Products and Processes*. Tokyo, Japan: Asian Productivity Organization, 1986.
- [27] P.-Y. Chou, J.-T. Tsai, and J.-H. Chou, "Modeling and optimizing tensile strength and yield point on a steel bar using an artificial neural network with taguchi particle swarm optimizer," *IEEE Access*, vol. 4, pp. 585–593, 2016.
- [28] Z. Wang, X. Li, S. Fang, and Y. Liu, "An accurate edge extension formula for calculating resonant frequency of electrically thin and thick rectangular patch antennas with and without air gaps," *IEEE Access*, vol. 4, pp. 2388–2397, 2016.
- [29] H. M. Hasanien, "Design optimization of PID controller in automatic voltage regulator system using Taguchi combined genetic algorithm method," *IEEE Syst. J.*, vol. 7, no. 4, pp. 825–831, Dec. 2013.
- [30] W. Sheng, P. Shan, J. Mao, Y. Zheng, S. Chen, and Z. Wang, "An adaptive memetic algorithm with rank-based mutation for artificial neural network architecture optimization," *IEEE Access*, vol. 5, pp. 18895–18908, 2017.
- [31] P. S. Oliveto, P. K. Lehre, and F. Neumann, "Theoretical analysis of rank-based mutation—Combining exploration and exploitation," in *Proc. IEEE Congr. Evol. Comput.*, May 2009, pp. 1455–1462.
- [32] H.-H. Chiang, K.-C. Hsu, and I.-H. Li, "Optimized adaptive motion control through an SoPC implementation for linear induction motor drives," *IEEE/ASME Trans. Mechatronics*, vol. 20, no. 1, pp. 348–360, Feb. 2015.
- [33] H.-J. Liu, K.-J. Li, W.-J. Lee, H. Gao, and Y. Sun, "Development of frequency variable inverter based on SOPC and Nios II," *IEEE Trans. Ind. Appl.*, vol. 49, no. 5, pp. 2237–2243, Sep. 2013.
- [34] C. A. Parmar, B. Ramanadham, and A. D. Darji, "FPGA implementation of hardware efficient adaptive filter robust to impulsive noise," *IET Comput. Digit. Techn.*, vol. 11, no. 3, pp. 107–116, 2016.
- [35] O. Gulbudak and E. Santi, "FPGA-based model predictive controller for direct matrix converter," *IEEE Trans. Ind. Electron.*, vol. 63, no. 7, pp. 4560–4570, Jul. 2016.



SENDREN SHENG-DONG XU (S'03–M'09–S'18) received the Ph.D. degree in electrical and control engineering from National Chiao Tung University, Hsinchu, Taiwan, in 2009. He is currently an Associate Professor with the Graduate Institute of Automation and Control, National Taiwan University of Science and Technology, Taipei, Taiwan. His current research interests include intelligent control systems, signal processing, image processing, and embedded systems.



HSU-CHIH HUANG (S'08–M'09–SM'18) received the Ph.D. degree in electrical engineering from National Chung-Hsing University, Taichung, Taiwan, in 2009. He is currently a Professor with the Department of Electrical Engineering, National Ilan University, Yilan, Taiwan. His current research interests include intelligent control, mobile robots, embedded systems, SoPC, and nonlinear control.



YU-CHIEH KUNG received the M.S. degree from the Graduate Institute of Automation and Control, National Taiwan University of Science and Technology, Taipei, Taiwan, in 2017. His research interests include intelligent control systems and embedded systems.



SHAO-KANG LIN is currently pursuing the M.S. degree with the Department of Electrical Engineering, National Ilan University. His current research interests include intelligent control, mobile robots, embedded systems, and SoPC.

...